

# Reactivity of C<sub>1</sub> Surface Species Formed in Methane Activation on Zn-Modified H-ZSM-5 Zeolite

Jian Feng Wu,<sup>[a]</sup> Wei David Wang,<sup>[a]</sup> Jun Xu,<sup>[b]</sup> Feng Deng,<sup>[b]</sup> and Wei Wang\*<sup>[a]</sup>

*Dedicated to Professor You Cheng Liu on the occasion of his 90th birthday*

**Abstract:** Solid-state <sup>13</sup>C magic angle spinning (MAS) NMR spectroscopy investigations identified zinc methyl species, formate species, and methoxy species as C<sub>1</sub> surface species formed in methane activation on the zeolite Zn/H-ZSM-5 catalyst at *T* ≤ 573 K. These C<sub>1</sub> surface species, which are possible intermediates in further transformations of methane, were prepared separately by adsorption of <sup>13</sup>C-enriched methane, carbon monoxide, and methanol onto zinc-containing catalysts, respectively. Successful isolation of each surface species allowed convenient in-

vestigations into their chemical nature on the working catalyst by solid-state <sup>13</sup>C MAS NMR spectroscopy. The reactivity of zinc methyl species with diverse probe molecules (i.e., water, methanol, hydrochloride, oxygen, or carbon dioxide) is correlated with that of organozinc compounds in organometallic chemistry. Moreover, surface formate and surface methoxy species pos-

sess distinct reactivity towards water, hydrochloride, ammonia, or hydrogen as probe molecules. To explain these and other observations, we propose that the C<sub>1</sub> surface species interconvert on zeolite Zn/H-ZSM-5. As implied by the reactivity information, potential applications of methane co-conversion on zinc-containing zeolites might, therefore, be possible by further transformation of these C<sub>1</sub> surface species with rationally designed co-reactants (i.e., probe molecules) under optimized reaction conditions.

**Keywords:** methane activation • reactivity • surface chemistry • zeolites • zinc

## Introduction

Activation and selective transformation of ubiquitous but inert C–H bonds represent two of the most challenging issues in modern chemistry.<sup>[1]</sup> Regarded as the “holy grail” in organometallic chemistry, C–H bond activation aims to provide atom-economic strategies in natural product and drug synthesis.<sup>[2,3]</sup> C–H bond activation is also directly connected to the possible utilization of light alkanes as feed-

stock compounds in the petroleum and natural gas industries.<sup>[4,5]</sup> Even in these industrial applications, catalytic conversion of methane into more valuable chemicals may, still, well be the most important and difficult task.<sup>[4,6]</sup>

Apart from approaches to the indirect conversion of methane via syngas,<sup>[7]</sup> numerous attempts have been devoted in the past decades to direct transformation of methane into more valuable products.<sup>[4,8–16]</sup> Recent investigations have implied that co-conversion<sup>[17–32]</sup> of methane and hydrocarbons/oxygenates on metal-containing (e.g., Ga, Zn, Mo, In, Ag, and Pt) zeolite catalysts could be promising processes performed at much lower temperatures under non-oxidative conditions. Rational development of these co-conversion processes will certainly benefit from the understanding of mechanisms involved in both methane activation and further transformation on the working catalysts. Motivated by this, pioneering work performed in the research groups of Baba,<sup>[20,33]</sup> Kazansky,<sup>[34]</sup> Ivanova,<sup>[35,36]</sup> and Stepanov<sup>[29,30]</sup> has been focusing on the spectroscopic identification of possible intermediates formed through C–H bond activation. For example, Stepanov and co-workers<sup>[29,30]</sup> observed C<sub>1</sub> surface species, such as zinc methyl, surface formate, and surface

[a] J. F. Wu, W. D. Wang, Prof. Dr. W. Wang  
State Key Laboratory of Applied Organic Chemistry  
College of Chemistry and Chemical Engineering  
Lanzhou University, Lanzhou, Gansu 730000 (P.R. China)  
Fax: (+86) 931 891 5557  
E-mail: wang\_wei@lzu.edu.cn

[b] Dr. J. Xu, Prof. Dr. F. Deng  
State Key Laboratory of Magnetic Resonance and Atomic and  
Molecular Physics, Wuhan Center for Magnetic Resonance  
Wuhan Institute of Physics and Mathematics  
Chinese Academy of Sciences, Wuhan 430071 (P.R. China)

Supporting information for this article is available on the WWW  
under <http://dx.doi.org/10.1002/chem.201002258>.

methoxy species during methane activation on zeolite Zn/H-BEA. Ivanova and co-workers<sup>[35]</sup> identified zinc methyl species after methane adsorption on Zn/MFI catalyst at ambient temperature. Accordingly, the reaction pathways for the formation of these  $C_1$  species have been proposed and extensively discussed<sup>[20,29,30,33–36]</sup> in terms of dissociative adsorption upon C–H bond activation of methane on the bifunctional catalysts.

Possible utilization of methane through co-conversion processes depends, however, on the chemical nature of initial intermediates generated during C–H bond activation, which governs further transformation of methane with diverse co-reactants. Therefore, investigations of the reactivity of possible  $C_1$  intermediates formed in methane activation are of great importance. This issue has recently been tackled by Stepanov and co-workers.<sup>[29,30]</sup> They demonstrated for the first time that surface methoxy species formed by dissociative adsorption of methane could methylate benzene on zeolite Zn/H-BEA.<sup>[29,30]</sup> Nevertheless, information on the reactivity of possible  $C_1$  intermediates is largely unknown in methane co-conversion. For example, although zinc methyl species have been consistently observed as  $C_1$  surface species in methane activation on zinc-modified zeolites, their reactivity has never been documented.

Solid-state NMR spectroscopy<sup>[37]</sup> is a powerful technique for the characterization of solid catalysts, especially in their functioning state.<sup>[38]</sup> We have long been interested in mechanistic investigations of heterogeneously catalyzed reactions by the use of solid-state NMR spectroscopy techniques.<sup>[39]</sup> The in situ stopped-flow magic angle spinning (MAS) NMR spectroscopy protocols<sup>[40–42]</sup> have allowed us to understand the nature of surface methoxy species in a variety of chemical transformation on acidic zeolite catalysts. In this contribution, similar strategies have been applied to clarify the reactivity of  $C_1$  surface species (i.e., zinc methyl species, surface formate species and surface methoxy species) formed in methane activation on Zn-modified H-ZSM-5 zeolite (denoted as Zn/H-ZSM-5). We first isolated each  $C_1$  surface species on the working catalyst and investigated its reactivity with different probe molecules (i.e., potential co-reactants in methane co-conversion) thereafter. Our results indicate that zinc methyl species, surface formate species and surface methoxy species possess distinct reactivity. Specifically, the reactivities of the zinc methyl species on zeolite Zn/H-ZSM-5 catalyst can be correlated with that of organozinc compounds in organometallic chemistry. We discuss the interconversion among these  $C_1$  surface species on the zeolite Zn/H-ZSM-5 catalyst.

## Results and Discussion

**Activation of methane on Zn/H-ZSM-5 catalyst at  $T = 473$ – $773$  K:** Figure 1 shows the  $^{13}\text{C}$  cross-polarization magic angle spinning (CP/MAS) NMR spectra recorded after activation of  $^{13}\text{C}$ -enriched methane ( $^{13}\text{CH}_4$ ) on zeolite Zn/H-ZSM-5 catalyst at reaction temperatures from 473 to 773 K. The re-

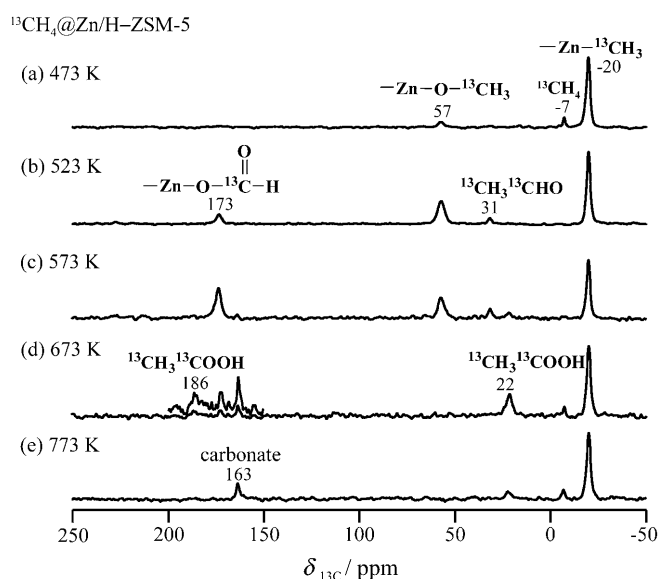


Figure 1.  $^{13}\text{C}$  CP/MAS NMR spectra recorded after  $^{13}\text{CH}_4$  activation on Zn/H-ZSM-5 catalyst for 20 min at  $T =$  a) 473, b) 523, c) 573, d) 673, and e) 773 K. The  $C_1$  surface species initially formed on the catalyst are zinc methyl species (at  $\delta = -20$  ppm), surface formate species (at  $\delta = 173$  ppm) and surface methoxy species (at  $\delta = 57$  ppm), respectively. Each spectrum was recorded with a spinning rate of 10.0 kHz.

sults are similar to those<sup>[29,30]</sup> obtained for methane activation on zeolite Zn/H-BEA. Methane activation on zeolite Zn/H-ZSM-5 has already started at 473 K, as evidenced by new signals observed in the  $^{13}\text{C}$  CP/MAS NMR spectrum (Figure 1 a). Apart from the  $^{13}\text{CH}_4$  signal at  $\delta = -7$  ppm, zinc methyl species (denoted as  $-\text{Zn}-^{13}\text{CH}_3$ ) appears at  $\delta = -20$  ppm<sup>[29,30,35,36]</sup> as the dominating signal and a surface methoxy species (denoted as  $-\text{Zn}-\text{O}-^{13}\text{CH}_3$ ) appears at  $\delta = 57$  ppm.<sup>[29,30]</sup> After methane activation at 523 K, surface formate species (denoted as  $-\text{Zn}-\text{OO}^{13}\text{CH}$ ) at  $\delta = 173$  ppm<sup>[29,30]</sup> and acetaldehyde ( $^{13}\text{CH}_3^{13}\text{CHO}$ ) at  $\delta = 31$  ppm<sup>[29,30]</sup> become evident (Figure 1 b). The signal intensity of the surface formate species at  $\delta = 173$  ppm exceeds that of the surface methoxy species at  $\delta = 57$  ppm after methane activation at 573 K (Figure 1 c) and both signals become invisible upon methane activation at higher temperatures (Figure 1 d and e). Upon methane activation from 573 to 773 K (Figure 1 c–e), small amounts of acetic acid ( $^{13}\text{CH}_3^{13}\text{COOH}$ ) and surface carbonate species<sup>[43,44]</sup> were also observed at  $\delta = 22$  ppm<sup>[29,30,45,46]</sup> and  $\delta = 163$  ppm,<sup>[47]</sup> respectively.

The  $C_1$  surface species initially formed during methane activation on zeolite Zn/H-ZSM-5 at  $T \leq 573$  K (Figure 1 a–c) are, therefore, zinc methyl species ( $^{13}\text{C}$  chemical shift of  $\delta = -20$  ppm), surface formate species ( $\delta = 173$  ppm) and surface methoxy species ( $\delta = 57$  ppm). These species may be involved in further transformation at higher reaction temperatures, as implied in the  $^{13}\text{C}$  CP/MAS NMR spectra shown in Figure 1 d and e. Possible pathways for the formation of these surface species on zeolite Zn/H-BEA have been suggested.<sup>[29,30]</sup> However, investigation of their reactivity, which may offer crucial information for further conversion of

methane on metal-containing zeolite catalysts, has not yet been achieved. Applying strategies similar to those for studying the reactivity of the surface methoxy species on acidic zeolites,<sup>[40–42]</sup> we isolated the above-mentioned species on the working catalysts and investigated their reactivity with different probe molecules. Typical results are presented in the following sections.

#### Reactivity of zinc methyl species on Zn/H-ZSM-5 catalyst:

As shown in Figure 1a, the dominating signal occurring upon methane activation at 473 K on Zn/H-ZSM-5 catalyst is that of zinc methyl species at  $-20$  ppm. By evacuation of unreacted methane after methane activation at a slightly lower temperature ( $T=453$  K), we were able to isolate the zinc methyl species on the Zn/H-ZSM-5 catalyst (see the Experimental Section for details). Figure 2a shows the  $^{13}\text{C}$  high-power proton decoupling (HPDEC) MAS NMR spectrum recorded after this procedure and the exclusive signal at  $-20$  ppm indicates the successful isolation of the

zinc methyl species on the Zn/H-ZSM-5 catalyst. The corresponding  $^{13}\text{C}$  CP/MAS NMR spectrum (not shown) is almost identical to Figure 2a, in which the signals for methane, surface methoxy or other species are absent. With the use of different probe molecules, the reactivity of the zinc methyl species on Zn/H-ZSM-5 catalyst was, therefore, investigated by solid-state  $^{13}\text{C}$  MAS NMR spectroscopy. Typical results are summarized in Scheme 1, which indicates that the chemical nature of the zinc methyl species on the Zn/H-ZSM-5 catalyst is similar to that of organozinc compounds<sup>[48–50]</sup> in organometallic chemistry.

Upon further heating of the zinc methyl species on Zn/H-ZSM-5 at 453 K for 20 min, a new signal due to  $^{13}\text{CH}_4$  appears at  $\delta = -7$  ppm in the  $^{13}\text{C}$  HPDEC MAS NMR spectrum, accompanied by a decrease of the signal of the zinc methyl species at  $\delta = -20$  ppm (Figure 2b). It has been proposed that the formation of the zinc methyl species originates from activation of methane on  $\text{Zn}^{2+}$  cations<sup>[35,36]</sup> or small  $\text{ZnO}^{[30]}$  clusters. Our result indicates that the zinc methyl species could be protonated back to methane and, therefore, the conversion of methane to the zinc methyl species is a reversible process on the Zn/H-ZSM-5 catalyst (Scheme 1a). As evidenced in Figure 2c–e, the conversion of the zinc methyl species back to methane on the Zn/H-ZSM-5 catalyst also occurs in the presence of other proton donors, such as water, methanol, and hydrochloride. The signal at  $\delta = -7$  ppm indicates the reoccurrence of methane on Zn/H-ZSM-5 catalyst when the zinc methyl species reacts with water at room temperature (Figure 2c), with methanol at 323 K (Figure 2d), or with hydrochloride at room temperature (Figure 2e). Methane was also reformed upon the reaction of the zinc methyl species and methanol at room temperature (not shown).

We propose that the high reactivity of the zinc methyl species in the presence of proton donors on zeolite Zn/H-ZSM-5 (Scheme 1a–d) can be understood on the basis of the similar chemistry of organozinc compounds.<sup>[48–50]</sup> For example, Coates<sup>[51]</sup> et al. showed that organometallic reagents are readily converted into hydrocarbons in the presence of water. Bruce<sup>[52]</sup> et al., Noltes and Boersma,<sup>[53]</sup> and Coates and Ridley<sup>[54]</sup> demonstrated that organozinc compounds can be transformed into organozinc alkoxide  $\text{RZnOR}'$  and hydrocarbons by alcoholysis. Furthermore, DFT calculations performed by Lambert<sup>[55,56]</sup> et al. have shed light on the mechanistic understanding of the reactions between methyl metal species ( $\text{M}-\text{CH}_3$ ) and hydrogen donors, such as,  $\text{NH}_3$ ,  $\text{H}_2\text{O}$ ,  $\text{HF}$ , and cyclopentadiene ( $\text{CpH}$ ).

The organozinc nature of zinc methyl species on the Zn/H-ZSM-5 catalyst has further been clarified in the reactions with oxygen and carbon dioxide. The  $^{13}\text{C}$  CP/MAS NMR spectrum shown in Figure 2f provides experimental evidence for the reaction of the zinc methyl species with oxygen at 523 K on zeolite Zn/H-ZSM-5. Together with the consumption of the zinc methyl species, the surface formate species (at  $\delta = 173$  ppm), surface methoxy species (at  $\delta = 57$  ppm), and methanol ( $^{13}\text{CH}_3\text{OH}$ , at  $\delta = 54$  ppm) are formed accordingly. In analogy to the classic carbanion reac-

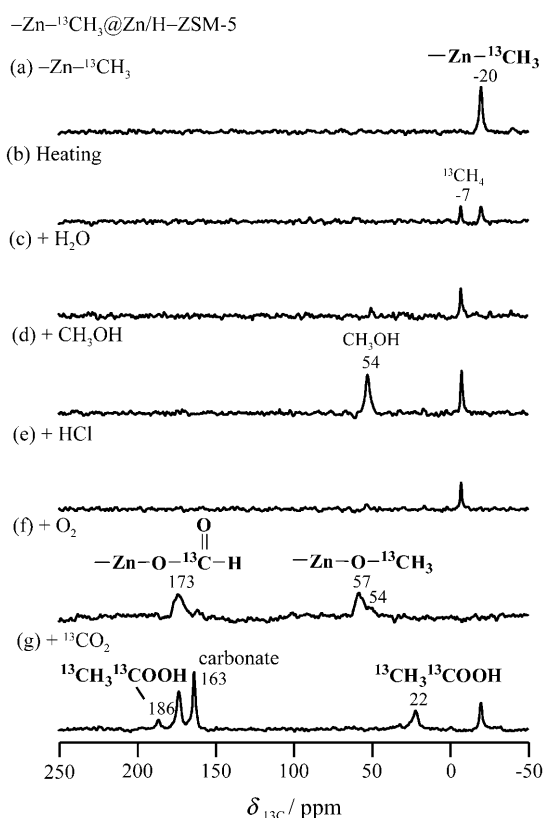
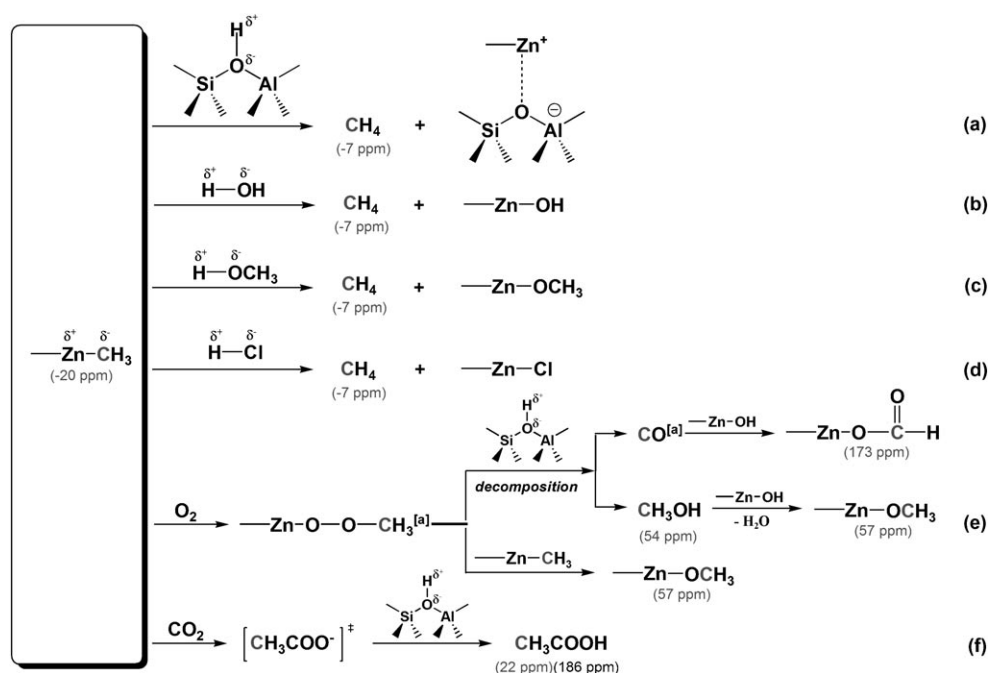


Figure 2. Reactivity of zinc methyl species ( $-\text{Zn}-^{13}\text{CH}_3$ , at  $\delta = -20$  ppm) on Zn/H-ZSM-5 catalyst evidenced by  $^{13}\text{C}$  HPDEC MAS NMR (a–e) and CP/MAS NMR (f and g) spectra: a) isolation of zinc methyl species (at  $\delta = -20$  ppm) by evacuation of unreacted  $^{13}\text{CH}_4$  after methane activation at 453 K; b) conversion of zinc methyl species to  $^{13}\text{CH}_4$  ( $-7$  ppm) upon further heating at 453 K for 20 min; c) reaction with water at room temperature; d) reaction with  $\text{CH}_3\text{OH}$  (45 mbar) at 323 K overnight; e) reaction with hydrochloride (32 mbar) at 298 K; f) reaction with oxygen (18 mbar) at 523 K for 20 min; g) reaction with  $^{13}\text{CO}_2$  (1 mbar) at 573 K for 20 min. Each spectrum was recorded with a spinning rate of 10.0 kHz. The reactivity of zinc methyl species on the Zn/H-ZSM-5 catalyst is summarized in Scheme 1.



Scheme 1. The reactivity of zinc methyl species ( $-\text{Zn}-\text{CH}_3$ ) on Zn/H-ZSM-5 catalyst. <sup>[a]</sup> Species that were not experimentally observed by  $^{13}\text{C}$  MAS NMR spectroscopy.

tions in organometallic chemistry, zinc methyl species may be reacting with oxygen to form methyl peroxy species first<sup>[57–59]</sup> (Scheme 1 e). The methyl peroxy species are further decomposed to carbon monoxide and methanol.<sup>[60]</sup> Surface formate species can, therefore, be generated from carbon monoxide (see below). The formation of surface methoxy species should be due either to the reaction of methyl peroxy species with zinc methyl species<sup>[52,53]</sup> or to the dehydration of methanol (Scheme 1 e). This mechanistic proposal is also supported by the previous investigation of Han<sup>[61,62]</sup> et al., who observed the formation of carbon monoxide and methanol in the direct partial oxidation (DPO) of methane on Zn-modified ZSM-5 catalysts.

The most interesting result comes from the reaction of zinc methyl species with carbon dioxide at 573 K on zeolite Zn/H-ZSM-5, which is shown in Figure 2 g. The formation of acetic acid is evidenced by the signals occurring at  $\delta = 186$  ppm (carbonyl group) and  $\delta = 22$  ppm (methyl group).<sup>[29,30,45,46]</sup> As depicted in Scheme 1 f, this observation can also be understood in analogy to the reaction of organozinc compounds with carbon dioxide.<sup>[63]</sup> Carbonate species (at  $\delta = 163$  ppm) are also formed due to the transformation of carbon dioxide alone on the working catalyst, which has been verified by adsorption of  $^{13}\text{C}$ -enriched carbon dioxide on zeolite Zn/H-ZSM-5 (Table S2 in the Supporting Information). It has been proposed that an equilibrium exists between surface formate species (at  $\delta = 173$  ppm) and carbonate species (at  $\delta = 163$  ppm) on a Cu/ZnO/Al<sub>2</sub>O<sub>3</sub> catalyst.<sup>[64]</sup>

**Reactivity of surface formate species on the Zn/H-ZSM-5 catalyst:** By evacuation of volatile products, we were able to isolate surface formate species ( $-\text{Zn}-\text{OO}^{13}\text{CH}$ ) on the Zn/H-

ZSM-5 catalyst after the reaction of  $^{13}\text{C}$ -enriched carbon monoxide at 573 K (see the Experimental Section for details and Figure S8 in the Supporting Information). Figure 3 a shows the  $^{13}\text{C}$  CP/MAS NMR spectrum recorded thereafter and the exclusive signal at  $\delta = 173$  ppm<sup>[29,30]</sup> indicates the successful isolation of surface formate species on the Zn/H-ZSM-5 catalyst. The analyses of  $^{13}\text{C}$  chemical shift parameters of the signal at  $\delta = 173$  ppm also confirmed the assignment as a surface formate species (Table S1 in the Supporting Information). With the use of different probe molecules, the reactivity of the surface formate species on the Zn/H-ZSM-5 catalyst was further investigated by solid-state  $^{13}\text{C}$  MAS NMR spectroscopy and the results are summarized in Scheme 2.

After further heating of the surface formate species on the Zn/H-ZSM-5 catalyst at 573 K for 20 min, the  $^{13}\text{C}$  HPDEC MAS NMR spectrum (Figure 3 b) indicates the decomposition of the surface formate species to carbon dioxide (at  $\delta = 126$  ppm<sup>[29,30]</sup>) and carbonate species (at  $\delta = 163$  ppm<sup>[47]</sup>). This result may be understood as the formation of carbon dioxide and hydrogen, possibly mediated by the decomposition of formic acid (HCOOH) (Scheme 2 a). Carbonate species are, therefore, formed from carbon dioxide, which has been confirmed by the control experiment on carbon dioxide on the Zn/H-ZSM-5 catalyst at 523 K (Table S2 in Supporting Information). Previous investigations of zinc oxide surfaces<sup>[43,65–67]</sup> also suggested that carbonate species could be formed by the reaction of carbon dioxide on defects. Moreover, Teichner and co-workers have identified the decomposition of surface formate species to carbon dioxide and hydrogen, and the formation of carbonate species on the surface of ZnO/ZrO<sub>2</sub> catalyst.<sup>[68]</sup>

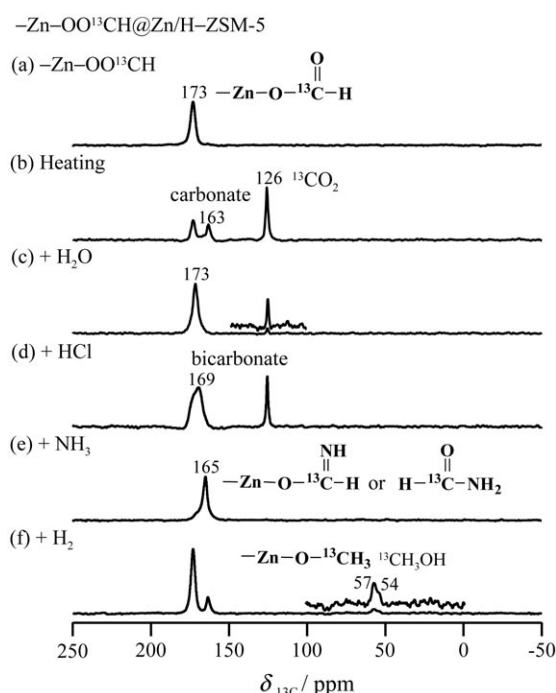
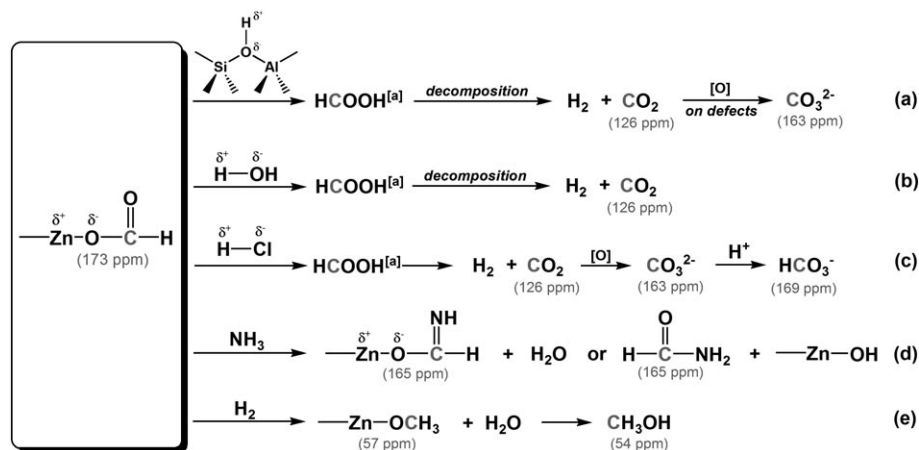


Figure 3. Reactivity of surface formate species (denoted as  $-\text{Zn}-\text{OO}^{13}\text{CH}$ ) on the Zn/H-ZSM-5 catalyst evidenced by the  $^{13}\text{C}$  CP/MAS NMR (a, e–f) and HPDEC MAS NMR (b–d) spectra: a) isolation of  $-\text{Zn}-\text{OO}^{13}\text{CH}$  species (at  $\delta=173$  ppm) by evacuation after  $^{13}\text{CO}$  activation on Zn/H-ZSM-5 catalyst at 573 K for 20 min; b) conversion of  $-\text{Zn}-\text{OO}^{13}\text{CH}$  species (at  $\delta=173$  ppm) to carbonate species (at  $\delta=163$  ppm) and carbon dioxide (at  $\delta=126$  ppm) upon further heating at 573 K for 20 min; c) reaction with water at room temperature; d) reaction with hydrochloride (75 mbar) at room temperature; e) reaction with ammonia (129 mbar) at 473 K for 20 min; and f) reduction of surface formate species by hydrogen (28 mbar) at 573 K for 20 min. Each spectrum was recorded with a spinning rate of 10.0 kHz. The reactivity of surface formate species on the Zn/H-ZSM-5 catalyst is summarized in Scheme 2.



Scheme 2. The reactivity of the surface formate species ( $-\text{Zn}-\text{OOCH}$ ) on Zn/H-ZSM-5 catalyst. a) Species that were not experimentally observed by  $^{13}\text{C}$  MAS NMR spectroscopy.

As shown in Figure 3c, the reaction of surface formate species with water on Zn/H-ZSM-5 catalyst at room temperature results in the formation of a small amount of carbon dioxide. Higher reaction temperatures increase the yield of

carbon dioxide (not shown). Teichner and co-workers also observed the decomposition of formate species into carbon dioxide and hydrogen on ZnO catalyst in the presence of water.<sup>[68]</sup> These findings suggest that carbon monoxide can be oxidized to carbon dioxide on Zn/H-ZSM-5 catalyst,<sup>[69]</sup> in which formate species may act as the key intermediates (Scheme 2b).

Figure 3d shows the  $^{13}\text{C}$  HPDEC MAS NMR spectrum recorded after the reaction of surface formate species with hydrochloride at room temperature. Carbon dioxide was observed as the main product. New species are also formed as a shoulder peak at about  $\delta=169$  ppm, which is assigned to bicarbonate.<sup>[47]</sup> As depicted in Scheme 2c, this reaction may also be understood as the formation of formic acid, which can be further transformed to carbonate and bicarbonate species.

Upon reaction of surface formate species and ammonia on the Zn/H-ZSM-5 catalyst at 473 K, new signal appears at 165 ppm in the recorded  $^{13}\text{C}$  CP/MAS NMR spectrum (Figure 3e). This signal is tentatively assigned to formimidate species. The same species were also formed on Zn/H-ZSM-5 catalyst when the reaction was carried out at 523 K (not shown). The formation of surface formimidate species may, therefore, be explained according to the formation of a Schiff base from aldehydes and amines (Scheme 2d). An alternative assignment of the signal at 165 ppm assumes that it is formamide, which originates from the attack of ammonia to the C–O bond of the surface formate species.

As shown in Figure 3f, reduction of surface formate species on Zn/H-ZSM-5 catalyst by hydrogen at 573 K gives products of surface methoxy species (at  $\delta=57$  ppm), carbonate species (at  $\delta=163$  ppm), and methanol (at  $\delta=54$  ppm), respectively. Similar results were also obtained on a zinc-containing catalyst<sup>[70]</sup> and other solid catalysts.<sup>[66,71–73]</sup> The

formation of surface methoxy species can be explained by the reduction of surface formate species with hydrogen (Scheme 2e). Carbonate species may come from surface formate species (see above), while the formation of methanol could come from surface methoxy species. Reduction of surface formate species on Zn/H-ZSM-5 catalyst by hydrogen at 773 K gives methane as additional product (not shown).

**Reactivity of surface methoxy species on ZnO catalyst:** Isolation of the surface methoxy species on zeolite Zn/H-ZSM-5

is not possible through methane activation due to the co-existence of zinc methyl species in large quantities (see above). Adsorption of methanol on zeolite Zn/H-ZSM-5 resulted in the formation of dimethyl ether, surface methoxy

species, and other surface species, which are hard to isolate from each other. By evacuation of the volatile species after methanol conversion (see the Experimental Section for details), we prepared the surface methoxy species on ZnO catalyst<sup>[47]</sup> as a model system to study the reactivity of the surface methoxy species on Zn/H-ZSM-5 catalyst. The dominating signal at  $\delta = 54$  ppm with spinning sidebands in Figure 4a is attributed to surface methoxy species isolated on

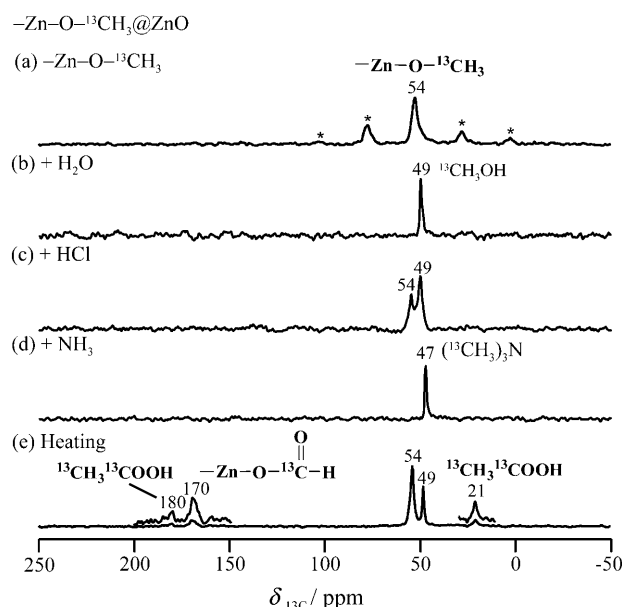


Figure 4. Reactivity of surface methoxy species on ZnO catalysts evidenced by the  $^{13}\text{C}$  CP/MAS NMR (a and e) and HPDEC MAS NMR (b–d) spectra: a) isolation of surface methoxy species (at  $\delta = 54$  ppm) by evacuation after methanol conversion on ZnO; b) reaction with water at room temperature; c) reaction with 68 mbar of hydrochloride at room temperature; d) reaction with 46 mbar of ammonia at room temperature; e) further transformation of surface methoxy species on ZnO upon heating at 353 K for 60 min. Asterisks denote spinning sidebands. The spectrum (a) was recorded with a spinning rate of 2.5 kHz and the others were recorded with that of 10.0 kHz. Surface methoxy species on a ZnO catalyst was applied as a model system for studying the reactivity of surface methoxy species on the zeolite Zn/H-ZSM-5. The reactivity of surface methoxy species on Zn-containing zeolites is summarized in Scheme 3.

the ZnO catalyst.<sup>[47]</sup> With the use of different probe molecules, the reactivity of the surface methoxy species on the ZnO catalyst was further investigated by solid-state  $^{13}\text{C}$  MAS NMR spectroscopy and the results are summarized in Scheme 3.

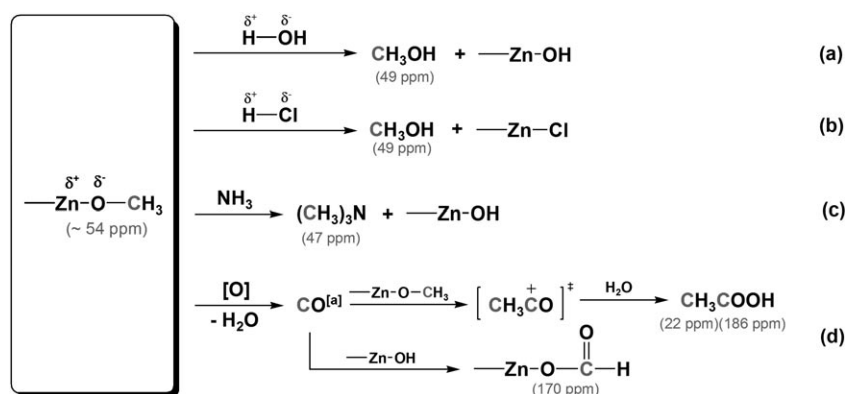
In analogy to those observed for surface methoxy species on acidic zeolites,<sup>[41]</sup> the reaction of surface methoxy species ( $\delta = 54$  ppm) with water on ZnO at room temperature gives metha-

nol ( $\delta = 49$  ppm<sup>[47]</sup>) as the product (Figure 4b and Scheme 3a). As shown in Figure 4c, the formation of methanol was also observed upon the reaction of surface methoxy species with hydrochloride on ZnO at room temperature (Figure 4c and Scheme 3b).

Figure 4d shows the  $^{13}\text{C}$  HPDEC MAS NMR spectrum recorded upon the reaction of surface methoxy species and ammonia on ZnO at room temperature. The signal at  $\delta = 47$  ppm can be attributed to the formation of trimethylamine,  $(\text{CH}_3)_3\text{N}$  (Scheme 3c). This assignment was further verified by loading of trimethylamine onto the ZnO catalyst (not shown). The formation of trimethylamine on ZnO (Scheme 3c) may also be rationalized as the result of the reaction of surface methoxy species and ammonia on acidic zeolites.<sup>[42]</sup>

Upon heating of the surface methoxy species on ZnO at 353 K for 60 min, acetic acid<sup>[29,30,45,46]</sup> was formed, evidenced by the signals at  $\delta = 180$  and  $\delta = 21$  ppm in the  $^{13}\text{C}$  CP/MAS NMR spectrum (Figure 4e). A weak signal also appears at  $\delta = 170$  ppm, which is assigned to the surface formate species.<sup>[29,30]</sup> The assignment of the surface formate species was verified by heating of  $^{13}\text{CO}$  on the ZnO catalyst (not shown). These findings imply that the surface methoxy species may be oxidized to carbon monoxide, which can further produce the surface formate species (see above) or follow the Koch-type reaction<sup>[42,74]</sup> to form acetic acid (Scheme 3d).

**Nature and interconversion of the C<sub>1</sub> surface species in methane activation on the zeolite Zn/H-ZSM-5 catalyst:** Zinc methyl species ( $-\text{Zn}-^{13}\text{CH}_3$ ), surface formate species ( $-\text{Zn}-\text{OO}^{13}\text{CH}$ ), and surface methoxy species ( $-\text{Zn}-\text{O}-^{13}\text{CH}_3$ ) are preliminary species observed during methane activation on zeolite Zn/H-ZSM-5 catalysts. Information on the chemical nature of these C<sub>1</sub> surface species will shed light on the design of co-reactants for further conversion of methane. Applying the strategies<sup>[40–42]</sup> for investigating the reactivity of surface methoxy species on acidic zeolites, we prepared these C<sub>1</sub> species separately by adsorption of  $^{13}\text{C}$ -enriched methane, carbon monoxide, or methanol onto zinc-containing catalysts. Successful isolation of each intermediate on



Scheme 3. The reactivity of methoxy species ( $-\text{Zn}-\text{O}-\text{CH}_3$ ) on ZnO catalyst. a) Species that were not experimentally observed by  $^{13}\text{C}$  MAS NMR spectroscopy.

the working catalyst allows us to further investigate their reactivity with different probe molecules by using solid-state NMR spectroscopy.

Being highly reactive due to the polarized carbon–metal ( $C^{\delta-}-M^{\delta+}$ ) bonds, organolithium, organomagnesium (Grignard), and organozinc compounds have been extensively used as very important organometallic reagents in organic synthesis.<sup>[48–50]</sup> For example, cross-coupling reactions of organozinc compounds with a variety of electrophiles offer novel strategies for chemo-, regio-, and stereoselective C–C bond formation.<sup>[75]</sup> More importantly, the formation and further transformation of organometallic species through C–H bond activation are often crucial steps for atom-economic approaches in natural product and drug synthesis.<sup>[2,3]</sup> On the other hand, as promising processes for methane utilization, co-conversion of methane with other reactants on metal-containing zeolite catalysts also involves C–H bond activation of methane and further transformation of  $C_1$  intermediate species. In this contribution, the reactivity of possible  $C_1$  intermediates formed through C–H bond activation of methane has been investigated and, specifically, the similarity of the reactivity of these surface species to that of organozinc compounds has been highlighted.

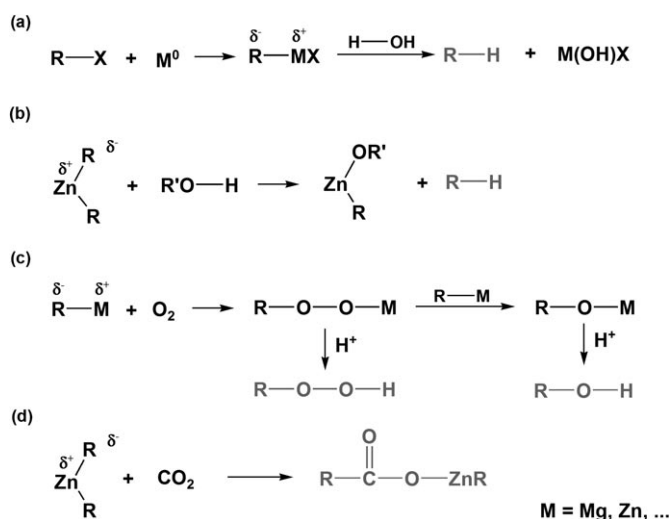
As revealed by the  $^{13}C$  MAS NMR investigations, zinc methyl species possess similar reactivity as that of organozinc compounds.<sup>[48–50]</sup> For example, zinc methyl species on zeolite Zn/H-ZSM-5 readily react with hydrogen donors to produce methane (Scheme 1 a–d). The reactions of dimethyl- or diethylzinc with various compounds containing reactive hydrogen were investigated by Coates et al.,<sup>[54]</sup> and followed by other groups.<sup>[52,53,55,56,76]</sup> Typical results obtained for the reactivity of organozinc compounds in organometallic chemistry are summarized in Scheme 4, in which the formation of hydrocarbons (R–H, such as methane) upon the reaction with water or alcohol was highlighted (Scheme 4 a and b). In our study, the reaction of zinc methyl species and

oxygen on zeolite Zn/H-ZSM-5 produces surface formate species, surface methoxy species, and methanol, which may be mediated by the formation of a methyl peroxy species (Scheme 1 e). As revealed by Abraham<sup>[57]</sup> and Knochel and co-workers,<sup>[58]</sup> oxidation of diethyl- and di-*n*-butylzinc gave alkyl peroxy species as the initial products, which could further react with excess of organometallic compounds to produce alcohols (Scheme 4 c). Most interestingly, we found that the reaction of zinc methyl species and carbon dioxide on zeolite Zn/H-ZSM-5 produces acetic acid (Scheme 1 f). A similar result was found by Inoue and Yokoo<sup>[63]</sup> for the reaction of diethylzinc and carbon dioxide (Scheme 4 d).

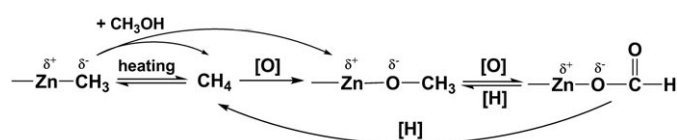
As revealed in this contribution, surface formate species could be prepared by the reaction of  $^{13}C$ -enriched carbon monoxide on zeolite Zn/H-ZSM-5 catalyst at 573 K. Further evacuation of other volatile products would retain the surface formate species as the sole species on the working catalyst, which makes further investigation of their reactivity feasible. In the case of surface formate species on zeolite Zn/H-ZSM-5 catalyst, the carbonyl groups can be easily reduced, by hydrogen, to surface methoxy species (Scheme 2) and further to methane. Schild et al. also observed that the formation of methane was correlated with the disappearance of formate species on zirconia-supported catalysts.<sup>[44]</sup> In analogy to formic acid, surface formate species on zeolite Zn/H-ZSM-5 are readily decomposed to carbon dioxide (Scheme 2). Our strategy for investigating the reactivity of surface formate species in methane activation may also be applicable to other catalytic processes (such as methanol synthesis<sup>[68,70,77]</sup> and the water-gas shift reaction<sup>[78]</sup>), in which surface formate species may act as the reactive intermediates.

It has well been demonstrated that an impregnated Zn/H-ZSM-5 catalyst contains sub-nanometric and macrocrystalline ZnO clusters.<sup>[79,80]</sup> For this reason, we use ZnO as the model catalyst for the zeolite Zn/H-ZSM-5 to prepare and isolate surface methoxy species. Surface methoxy species on zeolite Zn/H-ZSM-5 may possess comparable reactivity to the surface methoxy species<sup>[42]</sup> on acidic zeolites (Scheme 3). However, a discrepancy in reactivity for these two species exists in their reactions upon heating. Decomposition of surface methoxy species to hydrocarbons has consistently been observed on acidic zeolites H-Y, H-ZSM-5, and H-SAPO-34.<sup>[41]</sup> On the other hand, surface methoxy species on zinc-containing zeolites are readily oxidized to surface formate species as suggested by Stepanov and co-workers,<sup>[29,30]</sup> which was also confirmed in this contribution (Scheme 3 d). The  $^{13}C$  chemical shift of the surface methoxy species on the ZnO catalyst is about 54 ppm, which is 3 ppm less than that of surface methoxy species on Zn/H-ZSM-5 catalyst. This implies that the surface methoxy species on the zeolite Zn/H-ZSM-5 may be formed in the vicinity of both zinc and acidic sites.

The present solid-state NMR spectroscopy investigation also reveals the interconversion among the above-mentioned  $C_1$  surface species, which is depicted in Scheme 5. For example, a chemical equilibrium exists between methane



Scheme 4. The reactivity of organozinc compounds in organometallic chemistry with a) water,<sup>[53,78]</sup> b) alcohol,<sup>[54–56]</sup> c) oxygen,<sup>[59,60]</sup> and d) carbon dioxide.<sup>[65]</sup>



Scheme 5. Interconversion of C<sub>1</sub> surface species in methane activation on zeolite Zn/H-ZSM-5 catalyst.

and zinc methyl species on zeolite Zn/H-ZSM-5 at about 453 K (Figure 2a and b). Moreover, surface methoxy species formed during methane activation can be further oxidized to surface formate species (Figure 4e). On the other hand, surface formate species are easily reduced by hydrogen to surface methoxy species (Figure 3f) and further to methane on zeolite Zn/H-ZSM-5. Additionally, zinc methyl species could react with methanol to produce methane and surface methoxy species (Figure 2d).

In the absence of other co-reactants, zinc methyl species could only be converted back to methane on zeolite Zn/H-ZSM-5 without further transformation (Figure 2b). This observation is in accordance with previous reports on Zn/H-ZSM-5,<sup>[26]</sup> Mo-Zn/H-ZSM-5,<sup>[27]</sup> Cu-Zn/H-ZSM-5,<sup>[28]</sup> Zn<sup>2+</sup>/MFI,<sup>[36]</sup> and Zn/H-BEA<sup>[29,30]</sup> catalysts. Moreover, surface methoxy species on zeolite Zn/H-ZSM-5 would be oxidized to surface formate species (Figure 1b and Figure 4e), whereas the destiny of the surface formate species is to produce carbon dioxide (Figure 3b). All of these results re-emphasize the crucial existence of co-reactants for further conversion of methane to useful chemicals, which might be realized by certain reactions between the co-reactants and C<sub>1</sub> surface species. The zinc methyl species was identified as the most abundant surface species in methane activation on the Zn/H-ZSM-5 catalyst. The reactivity of the zinc methyl species on the working catalyst has been investigated in this contribution and, further correlated with that of organozinc compounds in organometallic chemistry.<sup>[48–50]</sup> This information may, therefore, shed new light on the understanding and further development of methane co-conversion process on zinc-containing zeolites.

## Conclusion

As has been seen for zeolite Zn/H-BEA,<sup>[29,30]</sup> zinc methyl species, surface formate species, and surface methoxy species were identified by us as initial C<sub>1</sub> surface species formed in methane activation on zeolite Zn/H-ZSM-5 catalyst. Applying similar strategies<sup>[40–42]</sup> for investigating the reactivity of surface methoxy species on acidic zeolites, we isolated these C<sub>1</sub> species and further investigated their reactivity by the use of different probe molecules. Our solid-state <sup>13</sup>C MAS NMR results indicate that zinc methyl species, surface formate species, and surface methoxy species formed by C–H bond activation of methane possess distinct reactivity in further transformations. For example, zinc methyl species show a reactivity similar to organozinc compounds in

organometallic chemistry<sup>[48–50]</sup>; surface formate species are formed from carbon monoxide and decomposed to carbon dioxide and hydrogen; and the reactivity of surface methoxy species is correlated with those of surface methoxy species on acidic zeolites.

In the absence of co-reactants, the destiny of zinc methyl species on zeolite Zn/H-ZSM-5 is to reform methane, whereas that of surface formate species or surface methoxy species is to produce carbon dioxide. Our investigation of the reactivity of C<sub>1</sub> surface species may, therefore, offer new information on further conversion of methane with co-reactants catalyzed by metal-modified zeolites. The distinct reactivity of C<sub>1</sub> species provides the possibility of selecting the co-reactants for methane co-conversion. For example, reactions of methane with either carbon monoxide or carbon dioxide give rise to acetic acid through different pathways: carbon monoxide reacts with surface methoxy species (Scheme 3d), and carbon dioxide reacts with zinc methyl species (Scheme 1f). More strikingly, the reaction of methane and carbon dioxide on zeolite Zn/H-ZSM-5 may be one way of converting greenhouse gases to useful chemicals.

## Experimental Section

**Materials and sample preparation:** As-synthesized zeolite Na-ZSM-5 (*n*<sub>Si</sub>/*n*<sub>Al</sub> = 15) was purchased from the Catalyst Plant of Nankai University, Tianjin, (P.R. China). <sup>13</sup>C-enriched methane (<sup>13</sup>C-enrichment of 99%) and carbon monoxide (<sup>13</sup>C-enrichment of 99%) were purchased from Spectra Gases. <sup>13</sup>C-enriched methanol (<sup>13</sup>C-enrichment of 99%) and carbon dioxide (<sup>13</sup>C-enrichment of 99%) were purchased from Cambridge Isotopes. All liquid reagents were degassed by three “freeze-pump-thaw” cycles before use and all gas reagents were used as received.

**Zeolite H-ZSM-5:** As-synthesized zeolite Na-ZSM-5 was calcined at 823 K in a muffle furnace for 6 h to remove the organic template. After calcination, a four-fold ion-exchange of zeolite Na-ZSM-5 to zeolite NH<sub>4</sub>-ZSM-5 was conducted at 353 K in a 1.0 M aqueous solution of NH<sub>4</sub>NO<sub>3</sub>. The zeolite NH<sub>4</sub>-ZSM-5 was then thoroughly washed in deionized water and dried at 353 K overnight. The residual Na content in zeolite NH<sub>4</sub>-ZSM-5 was 0.018 wt% determined by atomic absorption analysis (AAS). Zeolite NH<sub>4</sub>-ZSM-5 was then subjected to additional calcination at 823 K for 6 h in a muffle furnace leading to zeolite H-ZSM-5. The as-synthesized and template-free Na-ZSM-5 zeolites were characterized by XRD, and the acidic zeolite H-ZSM-5 obtained from zeolite NH<sub>4</sub>-ZSM-5 upon further activation in vacuum was characterized by multinuclear (<sup>1</sup>H, <sup>27</sup>Al, and <sup>29</sup>Si) solid-state NMR spectroscopy (Supporting Information).

**Zinc-modified H-ZSM-5 catalyst (Zn/H-ZSM-5):**<sup>[81]</sup> Zinc-modified zeolite H-ZSM-5 catalyst (denoted as Zn/H-ZSM-5) was prepared according to the literature<sup>[81]</sup> by impregnation of zeolite H-ZSM-5 with Zn(NO<sub>3</sub>)<sub>2</sub>. Typically, Zn(NO<sub>3</sub>)<sub>2</sub>·6H<sub>2</sub>O (0.292 g) was dissolved in deionized water (1.21 mL) and the aqueous solution obtained was added into zeolite H-ZSM-5 (1.00 g) with continuous stirring. The impregnated sample was dried in a rotary evaporator at 333 K for 0.5 h and treated in a muffle furnace at 673 K for 6 h, followed by further calcination in glass tubes in a vacuum (< 10<sup>−2</sup> mbar) for about 34 h (from 298 to 393 K with a heating rate of 1 K min<sup>−1</sup>; 393 K for 2 h to remove most of the water; then from 393 to 693 K with a heating rate of 0.7 K min<sup>−1</sup>; 693 K for 20 h). The dehydrated Zn/H-ZSM-5 catalyst was then subjected to reactant loading or sealed in situ for further use. AAS, XRD, UV/Vis, and multinuclear (<sup>1</sup>H, <sup>27</sup>Al, and <sup>29</sup>Si) solid-state NMR spectroscopy were applied to confirm the successful preparation of the Zn/H-ZSM-5 catalyst (Supporting Information). AAS results reveal that the Zn content in the catalyst is about 6.0–



6.2 wt %. The presence of ZnO on the external surfaces of the catalyst and ZnO cluster in the catalyst pores is shown by bands in the diffuse-reflectance spectrum at 370 and 265 nm, respectively.<sup>[79]</sup> X-ray diffraction, however, does not indicate the existence of macroscopic arrays of ZnO after this preparation.<sup>[79]</sup> All these results are consistent with those reported in the literature.<sup>[79,81]</sup>

**ZnO catalyst:** ZnO (Merck) was calcinated in glass tubes in a vacuum ( $<10^{-2}$  mbar) for about 28 h (from 298 to 393 K with a heating rate of 1 K min<sup>-1</sup>; 393 K for 2 h to remove most of the water; then from 393 K to 743 K with a heating rate of 0.6 K min<sup>-1</sup>; 743 K for 15 h). The dehydrated ZnO catalyst was then subjected to reactant loading or sealed in situ for further use.

**Methane activation on Zn/H-ZSM-5 catalyst:** A glass tube (outer diameter of about 6 mm and length of about 180 mm) containing around 130 mg of dehydrated Zn/H-ZSM-5 catalyst was loaded with about 50 mbar (approximately 0.19 mmol) of <sup>13</sup>CH<sub>4</sub> on a vacuum line and then flame-fused. After the reaction at a given temperature, the glass tube was cooled and opened in a glove box; and the catalyst was quickly transferred into a 4 mm MAS NMR rotor.

**Isolation of zinc methyl species on Zn/H-ZSM-5 catalyst:** Dehydrated Zn/H-ZSM-5 catalyst ( $\approx 130$  mg) was loaded with <sup>13</sup>CH<sub>4</sub> ( $\approx 50$  mbar) and heated at 323 K overnight for homogeneous adsorption. The sample was allowed to further react at 453 K for 45 min. Unreacted <sup>13</sup>CH<sub>4</sub> was then removed under vacuum for 20 min at room temperature to retain the zinc methyl species (denoted as -Zn-<sup>13</sup>CH<sub>3</sub>@Zn/H-ZSM-5) on the working catalyst. To explore their reactivity, the isolated zinc methyl species were subjected to further reactions with different probe molecules (e.g., water, methanol, hydrochloride, oxygen, or carbon dioxide) at given temperatures.

**Isolation of surface formate species on Zn/H-ZSM-5 catalyst:** Dehydrated Zn/H-ZSM-5 catalyst ( $\approx 130$  mg) was loaded with <sup>13</sup>CO ( $\approx 30$  mbar) and heated at 323 K overnight. The sample was allowed to further react at 573 K for 20 min. Volatile products were then removed under vacuum for 20 min at room temperature to retain the surface formate species (denoted as -Zn-OO<sup>13</sup>CH@Zn/H-ZSM-5) on the working catalyst. To explore the reactivity, the isolated surface formate species were subjected to further reactions with different probe molecules (e.g., water, hydrochloride, ammonia, or hydrogen) at given temperatures.

**Isolation of surface methoxy species on ZnO catalyst:** <sup>13</sup>CH<sub>3</sub>OH ( $\approx 100$  mbar) was allowed to react on the activated ZnO catalyst ( $\approx 300$  mg) at 298 K for 5 min. Unreacted <sup>13</sup>CH<sub>3</sub>OH was then removed under vacuum for 40 min at room temperature to retain the surface methoxy species (denoted as -Zn-O-<sup>13</sup>CH<sub>3</sub>@ZnO) on the working catalyst. To explore their reactivity, the isolated surface methoxy species were subjected to further reactions with different probe molecules (e.g., water, hydrochloride, or ammonia) at given temperatures.

**Solid-state <sup>13</sup>C MAS NMR experiments:** <sup>13</sup>C MAS NMR investigations were performed with a 4 mm Bruker MAS NMR spectroscopy probe on a Bruker Avance II WB 400 MHz spectrometer at a <sup>13</sup>C resonance frequency of 100.6 MHz. <sup>13</sup>C high-power proton decoupling (HPDEC) MAS NMR spectra were recorded after an excitation with a  $\pi/2$  pulse of 4.0  $\mu$ s and with a repetition time of 5 s. <sup>13</sup>C cross-polarization (CP) MAS NMR experiments were performed with a contact time of 3 ms and with a repetition time of 3 s. In these experiments, spectra were obtained with magic-angle spinning rates of 10.0, 8.0, and 2.5 kHz. All <sup>13</sup>C MAS NMR spectra were referenced to tetramethylsilane (TMS) and the precision of the <sup>13</sup>C chemical shift determinations is no greater than 1.0 ppm.

## Acknowledgements

This work was financially supported by the National Natural Science Foundation of China (nos.: 20602016 and 20933009) and the Key Grant Project of the Chinese Ministry of Education (no.: 309028).

[1] C. Copéret, *Chem. Rev.* **2010**, *110*, 656–680.

- [2] B. A. Arndtsen, R. G. Bergman, T. A. Mobley, T. H. Peterson, *Acc. Chem. Res.* **1995**, *28*, 154–162.
- [3] A. E. Shilov, G. B. Shul'pin, *Chem. Rev.* **1997**, *97*, 2879–2932.
- [4] J. H. Lunsford, *Catal. Today* **2000**, *63*, 165–174.
- [5] G. A. Olah, A. Molnar, *Hydrocarbon Chemistry*, 2nd ed., Wiley Interscience, New Jersey, **2003**.
- [6] R. H. Crabtree, *Chem. Rev.* **1995**, *95*, 987–1007.
- [7] T. V. Choudhary, V. R. Choudhary, *Angew. Chem.* **2008**, *120*, 1852–1872; *Angew. Chem. Int. Ed.* **2008**, *47*, 1828–1847.
- [8] A. Holmen, *Catal. Today* **2009**, *142*, 2–8.
- [9] L. Wang, L. Tao, M. Xie, G. Xu, J. Huang, Y. Xu, *Catal. Lett.* **1993**, *21*, 35–41.
- [10] Y. Xu, L. Lin, *Appl. Catal. A* **1999**, *188*, 53–67.
- [11] R. W. Borry III, Y. H. Kim, A. Huffsmith, J. A. Reimer, E. Iglesia, *J. Phys. Chem. B* **1999**, *103*, 5787–5796.
- [12] W. Ding, S. Li, G. D. Meitzner, E. Iglesia, *J. Phys. Chem. B* **2001**, *105*, 506–513.
- [13] W. Ding, G. D. Meitzner, D. O. Marler, E. Iglesia, *J. Phys. Chem. B* **2001**, *105*, 3928–3936.
- [14] S. Mukhopadhyay, A. T. Bell, *J. Am. Chem. Soc.* **2003**, *125*, 4406–4407.
- [15] S. Mukhopadhyay, A. T. Bell, *Angew. Chem.* **2003**, *115*, 1049–1051; *Angew. Chem. Int. Ed.* **2003**, *42*, 1019–1021.
- [16] S. Mukhopadhyay, A. T. Bell, *Angew. Chem.* **2003**, *115*, 3098–3101; *Angew. Chem. Int. Ed.* **2003**, *42*, 2990–2993.
- [17] V. R. Choudhary, A. K. Kinage, T. V. Choudhary, *Science* **1997**, *275*, 1286–1288.
- [18] V. R. Choudhary, K. C. Mondal, S. A. R. Mulla, *Angew. Chem.* **2005**, *117*, 4455–4459; *Angew. Chem. Int. Ed.* **2005**, *44*, 4381–4385.
- [19] T. Baba, H. Sawada, *Phys. Chem. Chem. Phys.* **2002**, *4*, 3919–3923.
- [20] T. Baba, Y. Iwase, K. Inazu, D. Masih, A. Matsumoto, *Microporous Mesoporous Mater.* **2007**, *101*, 142–147.
- [21] O. A. Anunziata, G. A. Eimer, L. B. Pierella, *Appl. Catal. A* **2000**, *190*, 169–176.
- [22] O. A. Anunziata, G. V. González Mercado, L. B. Pierella, *Catal. Lett.* **2003**, *87*, 167–171.
- [23] O. A. Anunziata, G. V. González Mercado, L. B. Pierella, *Catal. Commun.* **2004**, *5*, 401–405.
- [24] O. A. Anunziata, G. V. González Mercado, *Catal. Lett.* **2006**, *107*, 111–116.
- [25] G. V. Echevsky, E. G. Kodenev, O. V. Kikhtyanin, V. N. Parmon, *Appl. Catal. A* **2004**, *258*, 159–171.
- [26] H. T. Zheng, H. Lou, X. M. Zheng, *Cuihua Xuebao* **2004**, *25*, 255–256.
- [27] H. T. Zheng, H. Lou, Y. H. Li, J. H. Fei, Z. Y. Hou, Y. Xu, S. B. Wan, S. H. Wang, X. M. Zheng, *Gaodeng Xuexiao Huaxue Xuebao* **2005**, *26*, 285–289.
- [28] H. T. Zheng, H. L. Zhu, H. Lou, Z. Y. Hou, J. H. Fei, Y. H. Li, H. C. Xiao, Y. H. Yang, X. M. Zheng, *Cuihua Xuebao* **2005**, *26*, 49–54.
- [29] M. V. Luzgin, V. A. Rogov, S. S. Arzumanov, A. V. Toktarev, A. G. Stepanov, V. N. Parmon, *Angew. Chem.* **2008**, *120*, 4635–4638; *Angew. Chem. Int. Ed.* **2008**, *47*, 4559–4562.
- [30] M. V. Luzgin, V. A. Rogov, S. S. Arzumanov, A. V. Toktarev, A. G. Stepanov, V. N. Parmon, *Catal. Today* **2009**, *144*, 265–272.
- [31] D. B. Lukyanov, T. Vazhnova, *J. Mol. Catal. A* **2009**, *305*, 95–99.
- [32] J. Guo, H. Lou, X. Zheng, *J. Nat. Gas Chem.* **2009**, *18*, 260–272.
- [33] T. Baba, H. Sawada, T. Takahashi, M. Abe, *Appl. Catal. A* **2002**, *231*, 55–63.
- [34] V. B. Kazansky, A. I. Serykh, E. A. Pidko, *J. Catal.* **2004**, *225*, 369–373.
- [35] Y. G. Kolyagin, I. I. Ivanova, V. V. Ordonsky, A. Gedeon, Y. A. Pirogov, *J. Phys. Chem. C* **2008**, *112*, 20065–20069.
- [36] Y. G. Kolyagin, I. I. Ivanova, Y. A. Pirogov, *Solid State Nucl. Magn. Reson.* **2009**, *35*, 104–112.
- [37] C. Dybowski, S. Bai, *Anal. Chem.* **2008**, *80*, 4295–4300.
- [38] M. Hunger, W. Wang, *Adv. Catal.* **2006**, *50*, 149–225.
- [39] W. Wang, M. Hunger, *Acc. Chem. Res.* **2008**, *41*, 895–904.
- [40] W. Wang, M. Seiler, M. Hunger, *J. Phys. Chem. B* **2001**, *105*, 12553–12558.

- [41] W. Wang, A. Buchholz, M. Seiler, M. Hunger, *J. Am. Chem. Soc.* **2003**, *125*, 15260–15267.
- [42] Y. Jiang, M. Hunger, W. Wang, *J. Am. Chem. Soc.* **2006**, *128*, 11679–11692.
- [43] R. Lindsay, E. Michelangeli, B. G. Daniels, T. V. Ashworth, A. J. Limb, G. Thornton, A. Gutierrez-Sosa, A. Baraldi, R. Larciprete, S. Lizzit, *J. Am. Chem. Soc.* **2002**, *124*, 7117–7122.
- [44] C. Schild, A. Wokaun, A. Baiker, *J. Mol. Catal.* **1990**, *63*, 223–242.
- [45] M. V. Luzgin, M. S. Kazantsev, W. Wang, A. G. Stepanov, *J. Phys. Chem. C* **2009**, *113*, 19639–19644.
- [46] M. V. Luzgin, V. A. Rogov, N. S. Kotsarenko, V. P. Shmachkova, A. G. Stepanov, *J. Phys. Chem. C* **2007**, *111*, 10624–10629.
- [47] N. D. Lazo, D. K. Murray, M. L. Kieke, J. F. Haw, *J. Am. Chem. Soc.* **1992**, *114*, 8552–8559.
- [48] A. Boudier, L. O. Bromm, M. Lotz, P. Knochel, *Angew. Chem.* **2000**, *112*, 4584–4606; *Angew. Chem. Int. Ed.* **2000**, *39*, 4414–4435.
- [49] L. Pu, H. B. Yu, *Chem. Rev.* **2001**, *101*, 757–824.
- [50] R. E. Mulvey, *Organometallics* **2006**, *25*, 1060–1075.
- [51] G. E. Coates, M. L. H. Green, K. Wade, *Organometallic Compounds, Vol. 1*, Methuen & Co., London, **1967**.
- [52] J. M. Bruce, B. C. Cutsforth, D. W. Farren, F. G. Hutchinson, F. M. Rabagliati, D. R. Reed, *J. Chem. Soc. B* **1966**, 1020–1024.
- [53] J. G. Noltes, J. Boersma, *J. Organomet. Chem.* **1968**, *12*, 425–431.
- [54] G. E. Coates, D. Ridley, *J. Chem. Soc.* **1965**, 1870–1877.
- [55] C. Lambert, M. Kaupp, P. von R. Schleyer, *Organometallics* **1993**, *12*, 853–859.
- [56] C. Lambert, P. von R. Schleyer, *Angew. Chem.* **1994**, *106*, 1187–1199; *Angew. Chem. Int. Ed. Engl.* **1994**, *33*, 1129–1140.
- [57] M. H. Abraham, *J. Chem. Soc.* **1960**, 4130–4135.
- [58] I. Klement, H. Lütjens, P. Knochel, *Tetrahedron* **1997**, *53*, 9135–9144.
- [59] We once observed a <sup>13</sup>C NMR spectroscopy signal at  $\delta = 64$  ppm upon the reaction of methane and oxygen on Zn/H-ZSM-5 catalyst at 573 K. This signal might originate from the methyl peroxy, CH<sub>3</sub>OOH. The sample caused an explosion after the NMR spectroscopy measurement at room temperature, which might also imply the existence of peroxide species.
- [60] I. P. Fisher, C. F. H. Tipper, *Trans. Faraday Soc.* **1963**, *59*, 1174–1180.
- [61] S. Han, D. J. Martenak, R. E. Palermo, J. A. Pearson, D. E. Walsh, *J. Catal.* **1994**, *148*, 134–137.
- [62] S. Han, E. A. Kaufman, D. J. Martenak, R. E. Palermo, J. A. Pearson, D. E. Walsh, *Catal. Lett.* **1994**, *29*, 27–32.
- [63] S. Inoue, Y. Yokoo, *J. Organomet. Chem.* **1972**, *39*, 11–16.
- [64] Q. Sun, C. W. Liu, W. Pan, Q. M. Zhu, J. F. Deng, *Appl. Catal. A* **1998**, *171*, 301–308.
- [65] R. Davis, J. F. Walsh, C. A. Muryn, G. Thornton, V. R. Dhanak, K. C. Prince, *Surf. Sci.* **1993**, *298*, L196–L202.
- [66] J. Weigel, R. A. Koeppl, A. Baiker, A. Wokaun, *Langmuir* **1996**, *12*, 5319–5329.
- [67] Y. Wang, R. Kovacic, B. Meyer, K. Kotsis, D. Stodt, V. Staemmler, H. Qiu, F. Traeger, D. Langenberg, M. Muhler, C. Woll, *Angew. Chem.* **2007**, *119*, 5722–5725; *Angew. Chem. Int. Ed.* **2007**, *46*, 5624–5627.
- [68] D. Bianchi, T. Chafik, M. Khalfallah, S. J. Teichner, *Appl. Catal. A* **1993**, *105*, 223–249.
- [69] H. Berndt, G. Lietz, J. Völter, *J. Appl. Catal. A* **1996**, *146*, 365–379.
- [70] M. Bowker, H. Houghton, K. C. Waugh, *J. Chem. Soc. Faraday Trans. 1* **1981**, *77*, 3023–3036.
- [71] H. Abe, K.-i. Maruya, K. Domen, T. Onishi, *Chem. Lett.* **1984**, 1875–1877.
- [72] G. C. Chinchin, P. J. Denny, J. R. Jennings, M. S. Spencer, K. C. Waugh, *Appl. Catal.* **1988**, *36*, 1–65.
- [73] Y. Sun, P. A. Sermon, *J. Chem. Soc. Chem. Commun.* **1993**, 1242–1244.
- [74] A. G. Stepanov, M. V. Luzgin, V. N. Romannikov, K. I. Zamaraev, *J. Am. Chem. Soc.* **1995**, *117*, 3615–3616.
- [75] E. Erdik, *Tetrahedron* **1992**, *48*, 9577–9648.
- [76] G. Mehta, S. K. Kapoor, *J. Organomet. Chem.* **1974**, *66*, C33–C35.
- [77] M. Bowker, R. A. Hadden, H. Houghton, J. N. K. Hyland, K. C. Waugh, *J. Catal.* **1988**, *109*, 263–273.
- [78] R. Burch, *Phys. Chem. Chem. Phys.* **2006**, *8*, 5483–5500.
- [79] J. Chen, Z. Feng, P. Ying, C. Li, *J. Phys. Chem. B* **2004**, *108*, 12669–12676.
- [80] J. A. Biscardi, G. D. Meitzner, E. Iglesia, *J. Catal.* **1998**, *179*, 192–202.
- [81] A. G. Stepanov, S. S. Arzumanov, A. A. Gabrienko, A. V. Toktarev, V. N. Parmon, D. Freude, *J. Catal.* **2008**, *253*, 11–21.

Received: August 6, 2010

Published online: October 29, 2010